Rapid improvement in air quality due to aerosol-pollution control during 2012–2018: An evidence observed in Kunshan in the Yangtze River Delta, China

Junmei Wu, Yunjiang Zhang, Ting Wang, Yulin Qian

Rapid improvement in air quality due to aerosol-pollution control during 2012-2018: an evidence observed in Kunshan in the Yangtze River Delta, China

Junmei Wu[1], Yunjiang Zhang[2], Ting Wang[1], Yulin Qian[1]

[1]Kunshan Meteorological Administration, Kunshan, Jiangsu, China

[2]Laboratoire des Sciences du Climat et de l'Environnement (LSCE), CNRS-CEA-UVSQ, Université Paris-Saclay, Gif-sur-Yvette, France

Corresponding author:

Yunjiang Zhang (yunjiang.zhang@lsce.ipsl.fr) or Junmei Wu (wjmqingkong@126.com)

Abstract

China's severe air pollution was widely concerned in the past decade. A rigorous emission control has been implemented by the Chinese government since 2013. It is essential to evaluate changes of air pollutants to understand effectiveness of present air-pollution control on improving air quality. Here, we investigate temporal trends of air pollutants, including $PM_{2.5}$, SO_2, NO_2 and O_3, observed at 12 sites over the Kunshan area in the Yangtze River Delta region during 2012-2018 using Mann-Kendall statistical test. Overall, significant reduction trends of monthly $PM_{2.5}$ (-7.4% yr^{-1}) were observed, together with reduction in the $PM_{2.5}$ to CO ratio (-5.8% yr^{-1}), an indicator of secondary aerosol production. Secondary aerosol precursors, SO_2 (-10.3% yr^{-1}) and NO_2 (-4.4% yr^{-1}) also presented statistically significant reduction trends. These results reflect the consequence of emission control that leads to substantial reduction in the bulk $PM_{2.5}$ concentration, as well as secondary aerosols likely formed from SO_2 and NO_2. However, O_3 had statistically significant increase trend (+3.4% yr^{-1}) during 2014 – 2018. Limited formation of O_3 under high $PM_{2.5}$ and NO_2 concentrations

condition was found at daytime in summer, which might reflect one of the reasons causing the increase trend of O_3 under the current reduction scenario of $PM_{2.5}$ and NO_2. Potential source contribution function analysis demonstrated that the transport from the regions located to northwest of Kunshan could contribute to high concentrations of $PM_{2.5}$ in all seasons, while the south and southeast could be the high potential as source areas for O_3.

Keywords: Air quality, $PM_{2.5}$, O_3, trend, geographic origins, Yangtze River Delta

1. Introduction

Rapid industrialization and urbanization have been widely known as a key reason leading to air pollution, especially in developing countries. Air pollutants compose of various gases and particulate matter. Globally, fine aerosol particles ($PM_{2.5}$, with the aerodynamic diameter ≤ 2.5 μm) and ozone (O_3) are the major air pollutants in the present atmosphere. Both of them, $PM_{2.5}$ and O_3, have adverse health risks that can also result in human premature death (Shiraiwa et al., 2017;Dockery et al., 1996;Knowlton et al., 2004). As one of the largest developing countries in the world, China has experienced fast-developing economy and urbanization during the past decades, especially in the eastern China regions, like the Yangtze River Delta. However, this obviously brings a serious consequence being air pollution issues, such as extreme haze (Huang et al., 2014) and O_3 pollution (Li et al., 2019).

During the past decade, characterization of Chinese severe haze pollution and its formation mechanism have been widely studied (Sun et al., 2014;Huang et al., 2014;Guo et al., 2014;Ding et al., 2016;Zhang et al., 2017a;Sun et al., 2016a;Wang et al., 2016b;Cheng et al., 2016). As indicated by their findings, rapid formation of anthropogenic secondary fine aerosols over a regional scale is a dominated factor for the haze event formation under stagnant meteorological conditions. In the atmosphere, secondary fine aerosols are formed via the oxidation of their gaseous precursors, e.g., sulfur dioxide (SO_2), nitrogen oxides (NO_x), ammonia (NH_3) and volatile organic compounds (VOCs). To control haze formation and to further improve air quality, it is therefore necessary to reduce the budget of those aerosol precursors in the atmosphere (Cheng et al., 2019;Zhai et al., 2019). Several mankind emission source sectors, such as power plants, industry, transportation, agriculture, solvent use, residential activities, contribute to those aerosol precursors in China (Zheng et al., 2018). Since 2013, the China's Clean Air Action has been implemented to reduce emissions of air pollutants from these source sectors. As reported by Zheng et al. (2018), such emission control measure has successfully reduced some air pollutants, including SO_2 and NO_x by 59% and 21%, respectively, during 2013-2017. However, VOCs and NH_3 emissions were not expected to be reduced, and therefore remained stable for NH_3 and even increased for the VOCs during 2010–2017 (Zheng et al., 2018). Although the anthropogenic source emissions during recent years have been characterized in China, understanding of temporal trends of surface concentrations of those air pollutants and their geographic source distributions

remains limited. Investigation of long-term trends of those pollutants by ground-based measurements can help to further understand effectiveness and/or feedbacks of the air-pollution control progress on the improvement of air quality.

As one of the central cities in one of the core economic zones in eastern China, Kunshan is located in the region closed (around 100 km) to the megacity of Shanghai in the Yangtze River Delta region. Regarding to economic growth, Kunshan, with total area of approximately 900 square kilometers and around 1 million population, has ranked first among the 100 counties and cities for 13 years in China (as reported by Kunshan local chronicles Compilation Committee Office). By this rapid economic growth and the associated intensified urbanization process, the air pollution and other ecological and environmental problems have been increasingly prominent in the Kunshan region, and it has become one of four severe haze pollution zones in China. This fact poses a serious threat to urban development and the mutual restraint between economy and environment, causing wide social concern. In the present work, we quantified the temporal trends of air pollutants using Mann-Kendall test analysis, including $PM_{2.5}$, the $PM_{2.5}$ to CO ratio, SO_2, NO_2, and O_3, based on long-term ground-based measurements during 2012 – 2018 under different environments (including urban and near rural areas). Possible influence of regional and local pollution sources on the trends of those air pollutants was discussed. The potential influence of $PM_{2.5}$ changes on O_3 trends was explored. Geographic sources of those air pollutants were investigated using a potential source contribution function method.

2. Data and methods

2.1 Air pollutants dataset

Hourly data of air pollutants, including $PM_{2.5}$, O_3, NO_2, SO_2, and CO, were obtained from the online air quality monitoring network of Kunshan. There are 12 stations involved in this database, including 2 urban, 5 near rural, 3 town and 2 industrial sites, which has been summarized in Table S1. A meteorological parameter (i.e., wind speed) was obtained from a meteorological observation station in Kunshan.

2.2 Trend analysis

The Mann-Kendall statistical test (Mann, 1945), a non-parametric test, has been commonly used in time series analysis to identify the trends of observational datasets. In the Mann-Kendall test, the data don't have to meet the normality distribution, because non-parametric test works for all data distributions. This is a major advantage compared to parametric test, such as t test. The seasonal Mann-Kendall test is aiming to test the trend of the data with significant seasonality. In the present work, the trend analysis was performed on monthly mean data sets calculated from all, urban, and near rural sites, during the two periods, i.e., 2012 – 2018 and 2014 -2018, respectively. Before performing the Mann-Kendall test, the seasonality of the monthly data was firstly examined using the Kruskal-Wallis test (Kruskal and Wallis, 1952). If seasonality of the given data is significant (Kruskal-Wallis's $p < 0.05$), the seasonal Mann-Kendall test is applied, while the Mann-Kendall test will be applied for the data without significant seasonality (Kruskal-Wallis's $p > 0.05$). The median slope of the trend was calculated using Sen's slope method (Sen, 1968). The magnitude of the trends was presented only for the data with statistically significant trend at 5% significance level (see section 3.1). To examine the response of the China's rigorous air-pollution control (an Air Pollution Action Plan released in September 2013) to the improvement of air quality over a specific region, we compared these trends during the two periods of 2012-2018 and 2014-2018. The Mann-Kendal trend analysis was performed using a R trend package (Pohlert, 2018). Finally, the least-squares fitting method was also applied here to compare the Mann-Kendall statistical trend analysis results (see Tables S2-S4).

2.3 Potential geographic origins analysis

Potential source contribution function (PSCF) (Polissar, 1999) – a statistical approach – has been widely used to determine possible geographic origins of observed air pollutants. The PSCF describes the relationship between the coordinates of air mass back-trajectories and the ambient concentrations of air pollutants (Fleming et al., 2012). The magnitude of PSCF is defined as the grid-based probability linked to the pollutant origins, which is calculated by the ratio of m_{ij} to n_{ij}. m_{ij} represents the number of trajectory endpoints in a grid cell (*i,j*) associated with a given pollutant threshold value, and n_{ij} is the total count of trajectory endpoints. Therefore, the PSCF analysis allows us to understand the high potential source region that contributes the high concentration of air pollutants at the receptor site. To minimize a limitation of PSCF caused by a limited number of n_{ij} points in a grid cell, a downweighing function (w_{ij}) was performed here, as described in details by previous studies (Zhang et al., 2019b;Waked et al., 2014). In the present work, the PSCF analysis was performed based on 72-h back trajectory data that was calculated every 1 h using the HYSPLIT model (Draxler and Rolph, 2013) at an ending height of 100 m above ground level (a.g.l.). Global Data Assimilation System (GDAS) files with a 0.2° x 0.2° horizontal resolution were used here for the back-trajectory analysis. The receptor site was setting up at the near center (longitude: 120°8', latitude: 31°2') of Kunshan. The average concentrations of the air pollutants observed from all sampling sites were applied for the PSCF analysis. The threshold value of the ambient concentrations was set up at 75th percentile for the PSCF calculation, which is consistent with many previous studies (e.g., (Sun et al., 2015;Zhang et al., 2017b). All PSCF-related analysis was done here using an Igor-Pro user-friendly toolkit (ZeFir) (Petit et al., 2017).

3. Results and discussion

3.1 Trends and variations of major air pollutants

In China, the air-pollution control policies have been implemented by the Chinese government since 2010 (Zheng et al., 2018), while a new cleaner air action – so-called national "Ten Measures" – has been implemented to further improve the air quality since end of 2013 (Zhang et al., 2019a). Within such new clean air policies, the national emission standards have been applied for emission control linking to different source sectors (Zheng et al., 2018;Zhang et al., 2019a). For instance, the national standards GB 29620-2013, GB 4915-2013, and GB 13271-2014, were implemented to reduce some industrial sectors, i.e., Brick, Cement, and industrial boiler, respectively (Zheng et al., 2018). Instead of the Euro 3 standard, the Euro 4 standard was applied for diesel vehicle of transportation sector (Zheng et al., 2018). As a consequence of the 2013 cleaner air action, better air quality is logically expected, however ground-based measurements are needed to directly evaluate those pollution control policies. Figure 1 presents the trends in surface concentrations of $PM_{2.5}$, SO_2, NO_2, and O_3, as well as the ratio of $PM_{2.5}$ to CO measured at all sampling sites. As a result of Fig. 1a and Fig. S1a, $PM_{2.5}$ observed at all sampling sites (including urban, near rural, town, and industry areas), have an excellent consistency, suggesting the comparable surface mass concentrations of fine aerosols over the Kunshan region. During the both periods, i.e., 2012-2018 and 2014-2018, $PM_{2.5}$ exhibits statistically significant ($p < 0.05$) decreasing trends within 90 % confidence interval. For the average values calculated from all sites' observations, it can be noted that the change ratio (-8.2 % yr^{-1}) during 2014 – 2018 is higher than that of -7.4 % yr^{-1} during the whole period. Reduction in primary emissions of $PM_{2.5}$, by those mitigation measures (especially strength industrial emission standards) (Zheng et al., 2018;Zhang et al., 2019a), can partly explain the reduction trend of primary fractions of $PM_{2.5}$ observed in ambient air (Figure 1a). In fact, the reduction in total $PM_{2.5}$ can be overall due to reductions in both, primary and secondary aerosol fractions. To further explore the trends associated with secondary production of $PM_{2.5}$, an inert combustion tracer (CO) was applied to normalize the $PM_{2.5}$ mass concentrations (i.e., the $PM_{2.5}$-to-CO ratio) to minimize influence of primary combustion emissions (e.g., gasoline vehicles, coal combustion and biofuel burning) and meteorological dilution effect (de Gouw, 2005;Zhang and Cao, 2015;Hu et al., 2013;Sun

et al., 2016b). As Fig. 1b shows, the $PM_{2.5}$-to-CO ratios calculated with all sites datasets present significant decreasing trends for the both periods, which is roughly consistent with the $PM_{2.5}$ concentrations trends (Fig. 1a). These results could confirm that the significant reduction in $PM_{2.5}$ observed at a city level can be partly explained by the reduction of secondary production in $PM_{2.5}$. Those results reflect a fact of the enhanced role of the more rigorous air-pollution control in the reduction of fine aerosols in the atmosphere during the recent past years (Zheng et al., 2018), especially in the Yangtze River Delta region (Zhai et al., 2019).

Resulting in the reduction in secondary $PM_{2.5}$ fractions, another evidence of significant decreasing trends of SO_2 and NO_2 – gas-phase precursors of secondary inorganic aerosols – have been observed accordingly, as indicated by the results of Figs 1 c and d. It should be noted that the reduction ratios in the average SO_2 concentration (10.3 and 11.0 % yr^{-1} during 2012-2018 and 2014-2018, respectively) over all sites are approximately two times higher than those of the NO_2 (-4.4 and -5.8 % yr^{-1}). The features of SO_2 and NO_2 trends observed here are comparable to their emission trends for larger spatial scales on average, especially over mid-eastern China regions (Zheng et al., 2018;Zhang et al., 2019a). This may suggest that reduction in ambient SO_2 and NO_2 in a smaller region can be associated with those emission control policies over larger-regional scales. As reported by Zhang et al. (2019a), strength industrial emission standards are the largest contributor among some mitigation measures, including phase out small and polluting factories, phase out outdated industrial capacities, upgrades on industrial boilers, Promote clean fuels in the residential sector, and strengthen vehicle emission standards, to the reduction of air pollutants (i.e., SO_2 and NO_2, as well as $PM_{2.5}$) by the pollution control measures during the 2013-2017. Thus, reduction in SO_2 and NO_2 in Kunshan region can be made associated with those pollution control policies. Figures 2 a1 and b1 describe the relationship between the $PM_{2.5}$ to CO ratio and NO_2 and SO_2 observed in urban and near rural sites, which is characterized by higher ratio values associated with higher concentrations of both gaseous precursors. This implies that the high secondary $PM_{2.5}$ production in Kunshan could be partly explained by enhanced secondary inorganic aerosol formation from SO_2 and NO_2 chemistry in both urban and near-rural environments (Xie et al., 2015;Cheng et al., 2016;Wang et al., 2016a;Sun et al., 2016b). As shown in Figs. 2 a2 and b2, the ratios of NO_2 to SO_2 have increasing trends at both urban

and near-rural sites over recent years, suggesting an implication that NO_2-related aerosol chemistry might play a more important role in $PM_{2.5}$ pollution in the present and even future atmosphere. Interestingly, a higher ratio of NO_2 to SO_2 is observed at urban sites compared to that observed at near-rural sites (Figure 2), which is likely due to larger influence of transportation sectors on ambient NO_2 concentrations in urban environment. As presented in Figure 1d, there is no significant trend at 5% significance level for the mass concentration of NO_2 in urban environments, while significant decreasing trends are observed in near-rural environments during both periods, 2012-2018 and 2014-2018. This reflects that a more substantial influence of local emissions (e.g., traffic) on the ambient NO2 burden in urban environments rather than in near-rural environments. Moreover, the similar reduction rates (-7.8 % yr^{-1} versus -7.2 yr^{-1}) for near-rural sites during the two periods suggest a less effective emission control strategy by the new mitigation measures for the ambient NO_2 pollution control. As illustrated by Fig. S1d, the average mass concentration of NO_2 observed at urban sites is higher than that at near rural sites through the whole year, highlighting larger emissions of NO_2 in urban environments due to more intensive traffic emissions (i.e., transportation sector). Overall, these results above highlight the more effective control in SO_2 in the ambient air – mainly from industrial combustion sources – rather than NO_2 that is from transportation sources under the recent emission control policies (Zheng et al., 2018). Such feedback of the lack effectiveness of reduction in NO_2 to its corresponding secondary particulate production budget has been also observed by a very recent study, indicating a less change ratio of nitrate compared to sulfate during recent years in Nanjing (Ding et al., 2019).

For O_3 (see Fig. 1e and Table S2-S4), there is no statistically significant trend ($p>0.05$) for the period 2012-2018. Interestingly, there is a tendency for increasing O_3 concentrations (+3.4 % yr^{-1}, $p<0.05$) during 2014-2018. This indicates that the improvement in air quality in Kunshan is driven by reduction of the fine particles levels, while O_3 pollution becomes a more serious role in air pollution under the emission control strategies of China's clean air actions since 2013 (Zheng et al., 2018). O_3 is a secondary pollutant produced from photochemical oxidation of its precursors, i.e., volatile organic compounds (VOCs) and nitrogen oxides ($NOx = NO + NO_2$). Thus, the increasing trend in O_3 could be probably linked to feedbacks of the current air-pollution emission control, which will be further discussed in

section 3.2.

Since different sampling sites may present different environment features with, for instance, different source distributions. More intense local emissions (e.g., traffic and cooking) occur in urban region rather than in rural area. To further understand influence urban emissions on air quality, we compared the trends of air pollutants between urban and rural. Overall, the reduction ratios of $PM_{2.5}$ observed at near rural areas are generally higher than at urban areas for both periods (Fig. 1a). There is no statistically significant trend in the ratio of $PM_{2.5}$ to CO (Fig. 1b) and NO_2(Fig. 1d) for urban areas during the two periods. However, significant trends of NO_2 calculated from rural sites are observed during the two periods, the reduction ratios of which are higher than them for all sites. These results confirm the strong influence of local combustion source emissions on the trend variation at urban sites. Therefore, the less change in $PM_{2.5}$ in urban region could be linked to the more important impact of local primary emissions (i.e., traffic source) at urban sites rather than in the rural areas, which is actually comparable to limited change in $PM_{2.5}$ emitted from transportation sector during recent years (Zheng et al., 2018). The ratio of $PM_{2.5}$ to CO has significant decreasing trends for the both periods (Fig. 1b), which is consistent with the trends of O_3 with a higher change ratio at rural sites than in urban areas during the period of 2014-2018. This reflects that the ambient $PM_{2.5}$ composition in rural areas in Kunshan could be dominated by regional productions of secondary aerosols that are more sensitive to the regional-scale emission reduction control. SO_2 also presents decreasing concentrations with significant trend for both urban and rural areas, along with similar reduction ratios, suggesting a regional pollution characterization of SO_2 in Kunshan but with the lack influence of local sources emission.

Figure S2 illustrates comparison of diurnal cycles of air pollutants at different wind speed conditions (i.e., high and low WS, respectively) during the periods representing the beginning and end of the sampling years (i.e., 2012-2014 and 2016-2018, respectively). The thresholds to classify the high and low WS conditions are the average values of wind speed during nighttime in each season. The hourly data of air pollutants observed at all sampling sites were applied in this analysis. The objective of such data analysis is to roughly explore influence of regional- and local-dominated sources on air pollutants, which is similar as a previous study (Chambers et al., 2019). Regional and local pollution sources may be generally

associated with the high and low WS conditions, respectively. As presented in Fig. 3, the mass concentrations of air pollutants (including SO_2, NO_2 and $PM_{2.5}$) during 2012-2014 at both high and low WS conditions are higher than those during 2016-2018. Annual mean concentration of those pollutants at the two WS conditions have decreasing trends in each season, as illustrated by the results of Figure S3. Those results suggest that reduction in those pollutants in ambient air can be associated with both, local and regional emission control measures (Zheng et al., 2018;Zhang et al., 2019a). The diurnal cycles of SO_2 is characterized by a high peak in early morning in each season during 2012-2014 and 2016-2018 (Fig. S2a), which could be partly explained by enhanced anthropogenic emissions. NO_2 exhibits typical diurnal variations with two peaks at rush hours in early morning and evening (Fig. S2b) due to major influence of local traffic emissions. O_3 shows distinct diurnal cycles with maximum loadings at around noon in each season (Fig. S2c), because of strong solar radiation and significant photochemical production of O_3 during daytime.

As shown in Fig. S2d, $PM_{2.5}$ presents more complex diurnal patterns under different wind speed conditions in different seasons, since these variations are driven by very different compositions, sources, and evolution processes of $PM_{2.5}$ in different seasons, as well as meteorological conditions (Sun et al., 2015;Zhang et al., 2015b;Cheng et al., 2019). The concentration of $PM_{2.5}$ at the low WS condition is higher than that at the high WS condition (Figs. S2d and S3c), which could be explained by local primary emissions and enhanced secondary aerosol productions, as well as less impact of atmospheric dilution at near-stagnant meteorological conditions on loadings of atmospheric aerosols. The ratio of $PM_{2.5}$ to CO at the low WS condition is also higher than that at the high WS condition in different periods and seasons (Fig. S3d), which may further support enhanced secondary fine aerosol formation at the low WS conditions. This can be also supported by higher SO_2 and NO_2– gas-phase precursors of secondary inorganic $PM_{2.5}$ that accounts for a large fraction of $PM_{2.5}$ mass in the Yangtze River delta (Huang et al., 2012;Zhang et al., 2015c;Zhang et al., 2015b;Zhang et al., 2017a) – at the low WS conditions (Fig. S3a and S3b). Those results are also consistent with previous findings that formation of haze pollution events occurs more frequently under stagnant meteorological conditions in the eastern China regions (Sun et al., 2016a;Sun et al., 2014;Ding et al., 2016;Zhang et al., 2017a). As shown in Fig. S3, the mass concentration of $PM_{2.5}$ and the ratio of $PM_{2.5}$ to CO display decreasing trends at both low and

high WS conditions in each season, suggesting positive influence of regional and local pollution controls on reduction in ambient $PM_{2.5}$ in the Kunshan region. The detailed reasons leading to these variations can be further investigated with aerosol chemical speciation measurements and source apportionment, which however were not achieved by the present study.

3.3 Relationship between $PM_{2.5}$ and O_3 in summer

The increasing trends of O_3 have been discussed in the section above. As shown in Fig. 1e, the significant enhancement of O_3 concentrations are observed during summertime in each year, indicative of more health risk of O_3 occurring in summer in the recent years. We therefore further investigated the possible reasons increasing O_3 in summer and whether this increase is linked to the $PM_{2.5}$ concentration variations and its precursors reductions during the recent years.

Figure 3 shows the relation between O_3 and $PM_{2.5}$ at different NO_2 concentrations conditions at daytime in summer. It can be clearly seen that there is a positive relationship between O_3 against $PM_{2.5}$ at lower NO_2 levels (< around 20 – 30 μg m^{-3}). This suggests that the photochemical chemistry can account for increases in the summertime $PM_{2.5}$ production to a certain extent. However, O_3 presents very limited change in concentrations as increase of $PM_{2.5}$ at higher NO_2 levels (> around 30 μg m^{-3}) (see Figs. 3 and S4). This describes a phenomenon of limited formation of O_3 under higher NO_2 conditions, which might suggest that reduction in NOx concentrations could be one of the reasons leading to increase of O_3 production. In fact, several recent previous studies have also found such a possible reason based on field measurements (Xu et al., 2019) and modeling simulations (Li et al., 2019). Furthermore, Xu et al. (2019) suggested that O_3 production was in a VOC-limited regime in the downtown and sub-urban areas in Shanghai –near our study area. Modeling results achieved by a chemical transport model (GEOS-Chem) simulation also suggested that O_3 production in megacity cluster in the Yangtze River Delta was VOC-limited (Li et al., 2019).

The presence of aerosol particles can influence photochemical reactions in the atmosphere (Li et al., 2019), since complex aerosol chemistry could act as a sink of

atmospheric oxidants, e.g., OH radical, hydrogen peroxide (H_2O_2), and O_3 (Fu et al., 2019). In the atmosphere, these oxidants can react with aerosol precursors (e.g., SO_2, NO_2 and VOCs) to form secondary aerosol particles (Zhang et al., 2015a), and thus these oxidants are depleted via such aerosol formation processes. As Fig. 3 shows, the higher ratio of $PM_{2.5}$ to CO – an indicator of secondary aerosol production – is observed corresponding to the high $PM_{2.5}$ concentrations for the scenario of the O_3 versus $PM_{2.5}$ under high NO_2 concentrations levels. This result could theoretically suggests that changes in ambient concentrations of $PM_{2.5}$ and its precursors have considerable influence on O_3 concentrations levels (Li et al., 2019;Fu et al., 2019). As indicated by Li et al. (2019), rapid reduction in surface $PM_{2.5}$ concentrations could result in a slowing down sink of hydroperoxy (HO_2) radicals and thereby increase in O_3 production. Hence, our observational results could be partly explained by such a mechanism leading to the increasing trend of O_3 observed during the recent years (Li et al., 2019).

3.4 Geographic sources

Figure 4 shows the seasonal characterization of the potential source areas for $PM_{2.5}$, the $PM_{2.5}$ to CO ratio, SO_2 and NO_2. As shown in Fig. 4a, $PM_{2.5}$ shows a similar source region characterized by a high PSCF band along Hengshui-Xuzhou-Hefei-Nanjing-Shanghai in all seasons. These results are generally consistent with the high potential source areas of the $PM_{2.5}$ to CO ratio (Fig. 4b), suggesting that regional transport of secondary aerosol productions from the northwest may play a dominant role in formation of severe winter haze pollution in Kunshan. Besides of that, the contribution from local areas near Kunshan to the $PM_{2.5}$ pollution cannot be ignored in each season (Fig. 4a). Meanwhile, a similar potential source area for SO_2 is also observed in winter, spring and fall, as indicated by Fig. 4c, which is characterized by a broader band and even longer regional transport pathways up to Hebei Province, one of the most polluted regions in China caused by intense emissions of coal combustion (Wang et al., 2018;Koukouli et al., 2018;Tian et al., 2010). In summer, high PSCF region of SO_2 is mainly dominated by local scale (Fig. 4c), which is similar as the PSCF distributions for NO_2 (Fig. 4d), as well as the ratio of $PM_{2.5}$ to CO with higher PSCF values over the Yangtze River Delta region (Fig. 4a). These results indicate the importance of local

sources emissions for $PM_{2.5}$ pollution in summer. Compared to SO_2 in other seasons (i.e., winter, spring, and fall), a relative narrow source area located at northwest and southwest and is observed for NO_2 (Fig. 4d), which is indicative of a regional transport contribution to NO_2 in addition to local emissions. Those results highlight again the importance of controlling NO_2 and SO_2 emissions over a region scale in reduction of ambient $PM_{2.5}$ burden. According to Fig. S5, showing the year-round PSCF of $PM_{2.5}$, SO_2, and NO_2, as well as the ratio of $PM_{2.5}$ to CO, all air pollutants in each year show similar PSCF spatial distributions, suggesting a common characteristic of the potential sources in winter every year. Thus, regional transport from these areas (i.e., northwest) and emissions over local-scale regions play an important role in the formation of haze pollution in the region near Shanghai during the whole investigation period 2011 - 2018.

Figure 5 presents the spatial distributions of PSCF values for O_3 in all seasons, which are overall characterized by high potential source region located in southwestern, southern, and southeastern areas, e.g., Hangzhou-Shanghai. This suggests that air masses origins from these regions could have potentially important impact on O_3 formation observed in the Kunshan region. In the warm months, higher concentrations of O_3 are frequently observed in each year (Fig. 1e). These distinct PSCF regions located in southeastern region could then explain the possible source origins of O_3 episodes occurred in summer and spring. Moreover, the PSCF characteristics of O_3 are comparable among each year, as indicated by the summertime results of Fig. S6. Given that many cities are located in the high potential PSCF of O_3, the transport of air masses from these areas would have a potentially high impact on the formation of O_3 pollution episodes in the region near Shanghai in summer. Therefore, the combination of emissions control of NOx and VOCs in a regional scale, such as over megacity cluster area, could help to improve the summertime air pollution caused by O_3.

4. Conclusion

We conducted a comprehensive analysis in long-term and multi-site dataset of air pollutants (including $PM_{2.5}$ and O_3) observed in Kunshan during the period of 2012-2018. The trends of those air pollutants were calculated using Mann-Kendall statistical test. The monthly $PM_{2.5}$ averaged from all sites data presented statically significant reduction trend (-7.4% per year)

during 2012-2018. The ratio of $PM_{2.5}$ to CO also had a significant reduction trend for the averages of all sites, which is consistent with the $PM_{2.5}$, suggesting the possible reduction of secondary aerosol production during the past several years. This possibility is supported by the significant reduction trend of aerosol precursors, SO_2 (-10.3% per year) and NO_2 (-4.4% per year). Such higher change ratio of SO_2 suggested a more effective emission control strategy for atmospheric SO_2 burden than for NO_2. However, there was no significant trend for NO_2 observed at urban sites, emphasizing the importance of local traffic emissions for the temporal variations of NO_2. Interestingly, O_3 presented significant increase trend (+3.5% per year) during the period of 2014-2018. Enhanced formation of O_3 was observed to be associated with lower $PM_{2.5}$ and NO_2 concentrations during daytime in summer, which implies that the current emission control might provide favorable environment conditions (e.g., low $PM_{2.5}$ loadings) for O_3 formation. The geographic origins of air pollutants were investigated using PSCF analysis, which presented different source regions between $PM_{2.5}$ and O_3 across different seasons. Higher potential source areas for $PM_{2.5}$ were located to the northwest of Kunshan in all seasons, while the south and southeast were the major geographic origins of O_3 especially in spring and summer. Overall, these results demonstrated that improvement of air quality was due to reduction in the concentration level of $PM_{2.5}$, along corresponding reduction in its precursors of SO_2 and NO_2 during the past years. Effective and well balanced controls are needed to further reduce both, ambient $PM_{2.5}$ and O_3 pollution, especially over urban areas.

Acknowledgement

This work is supported by the scientific research program of Suzhou Meteorological Bureau (SZKJ201707). We thank Kunshan Environmental monitoring center for supporting the observation data.

Conflicts of Interest

The authors declare no conflict of interest.

Figure captions

Figure 1. Monthly trends in (**a**) $PM_{2.5}$, (**b**) $PM_{2.5}$-to-CO ratio, (**c**) NO_2, (**d**) SO_2, and (**e**) O_3. Two methods (see Tables S2-S4), including Mann-Kendall test and least-squares fitting, have been applied for the time series statistical analysis aiming to quantify the trends over the two periods, i.e., A (2012-2018) and B (2014-2018), respectively. Note that the trend was not further quantified for the data without statistically significant trend according to the Mann-Kendall test.

Figure 2. Daily ratio between NO_2 and SO_2 as a function of (**a**) the measuring dates and (**b**) the $PM_{2.5}$ to CO ratio, at urban and near rural sites, respectively.

Figure 3. Relationship between hourly O_3 and $PM_{2.5}$ at different NO_2 concentrations conditions at daytime (10:00 – 17:00) in summer (June-July-August) during 2012-2018. The relationship between O_3 and $PM_{2.5}$ are averaged (square-shaped points) based on the levels of NO_2 concentrations, where error bars indicate standard deviations. Hourly average data points (circle points) are color-scaled by date during the entire period, and size-scaled by the $PM_{2.5}$ to CO ratio.

Figure 4. Seasonal potential source regions of (**a**) $PM_{2.5}$, (**b**) the $PM_{2.5}$ to CO ratio, (**c**) SO_2, and (**d**) NO_2, which were achieved from PSCF analysis during wintertime. The cities marked in each panel are Beijing (BJ), Shijiazhuang (SJZ), Weifang (WF), Jinan (JN), Hefei(HF), Xuzhou(XZ), Nanjing(NJ), Shanghai(SH), Hangzhou(HZ), Nanchang(NC), and Wenzhou(WZ), Fuzhou(FZ). Shijiazhuang (SJZ), and Hengshui (HS). The color scales refer to the PSCF values. The point in red in each panel represents the location of this study.

Figure 5. Seasonal potential source regions of O_3: (**a**) winter; (**b**) spring; (**c**) summer; and (**d**) fall. The cities marked in each panel are same as Figure 5. The color scales refer to the PSCF

441 values. The point in red in each panel represents the location of this study.

442

References

Chambers, S. D., Podstawczyńska, A., Pawlak, W., Fortuniak, K., Williams, A. G., and Griffiths, A. D.: Characterizing the State of the Urban Surface Layer Using Radon-222, Journal of Geophysical Research: Atmospheres, 124, 770-788, 10.1029/2018jd029507, 2019.

Cheng, J., Su, J., Cui, T., Li, X., Dong, X., Sun, F., Yang, Y., Tong, D., Zheng, Y., Li, Y., Li, J., Zhang, Q., and He, K.: Dominant role of emission reduction in PM2.5 air quality improvement in Beijing during 2013–2017: a model-based decomposition analysis, Atmos. Chem. Phys., 19, 6125-6146, 10.5194/acp-19-6125-2019, 2019.

Cheng, Y., Zheng, G., Wei, C., Mu, Q., Zheng, B., Wang, Z., Gao, M., Zhang, Q., He, K., Carmichael, G., Pöschl, U., and Su, H.: Reactive nitrogen chemistry in aerosol water as a source of sulfate during haze events in China, Sci. Adv., 2, 10.1126/sciadv.1601530, 2016.

de Gouw, J. A.: Budget of organic carbon in a polluted atmosphere: Results from the New England Air Quality Study in 2002, J. Geophys. Res., 110, 10.1029/2004jd005623, 2005.

Ding, A., Huang, X., Nie, W., Chi, X., Xu, Z., Zheng, L., Xu, Z., Xie, Y., Qi, X., Shen, Y., Sun, P., Wang, J., Wang, L., Sun, J., Yang, X. Q., Qin, W., Zhang, X., Cheng, W., Liu, W., Pan, L., and Fu, C.: Significant reduction of PM2.5 in eastern China due to regional-scale emission control: Evidences from the SORPES station, 2011-2018, Atmos. Chem. Phys. Discuss., 2019, 1-21, 10.5194/acp-2019-407, 2019.

Ding, A. J., Huang, X., Nie, W., Sun, J. N., Kerminen, V. M., Petäjä, T., Su, H., Cheng, Y. F., Yang, X. Q., Wang, M. H., Chi, X. G., Wang, J. P., Virkkula, A., Guo, W. D., Yuan, J., Wang, S. Y., Zhang, R. J., Wu, Y. F., Song, Y., Zhu, T., Zilitinkevich, S., Kulmala, M., and Fu, C. B.: Enhanced haze pollution by black carbon in megacities in China, Geophys. Res. Lett., 43, 2873-2879, 10.1002/2016GL067745, 2016.

Dockery, D. W., Cunningham, J., Damokosh, A. I., Neas, L. M., Spengler, J. D., Koutrakis, P., Ware, J. H., Raizenne, M., and Speizer, F. E.: Health effects of acid aerosols on North American children: respiratory symptoms, Environmental Health Perspectives, 104, 500-505, 10.1289/ehp.96104500, 1996.

Fu, Y., Liao, H., and Yang, Y.: Interannual and Decadal Changes in Tropospheric Ozone in China and the Associated Chemistry-Climate Interactions: A Review, Advances in Atmospheric Sciences, 36, 975-993, 10.1007/s00376-019-8216-9, 2019.

Guo, S., Hu, M., Zamora, M. L., Peng, J., Shang, D., Zheng, J., Du, Z., Wu, Z., Shao, M., Zeng, L., Molina, M. J., and Zhang, R.: Elucidating severe urban haze formation in China, Proc. Natl. Acad. Sci. U.S.A., 111, 17373-17378, 10.1073/pnas.1419604111, 2014.

Hu, W. W., Hu, M., Yuan, B., Jimenez, J. L., Tang, Q., Peng, J. F., Hu, W., Shao, M., Wang, M., Zeng, L. M.,

Wu, Y. S., Gong, Z. H., Huang, X. F., and He, L. Y.: Insights on organic aerosol aging and the influence of coal combustion at a regional receptor site of central eastern China, Atmos. Chem. Phys., 13, 10095-10112, 10.5194/acp-13-10095-2013, 2013.

Huang, R. J., Zhang, Y., Bozzetti, C., Ho, K. F., Cao, J. J., Han, Y., Daellenbach, K. R., Slowik, J. G., Platt, S. M., Canonaco, F., Zotter, P., Wolf, R., Pieber, S. M., Bruns, E. A., Crippa, M., Ciarelli, G., Piazzalunga, A., Schwikowski, M., Abbaszade, G., Schnelle-Kreis, J., Zimmermann, R., An, Z., Szidat, S., Baltensperger, U., El Haddad, I., and Prevot, A. S.: High secondary aerosol contribution to particulate pollution during haze events in China, Nature, 514, 218-222, 10.1038/nature13774, 2014.

Huang, X. F., He, L. Y., Xue, L., Sun, T. L., Zeng, L. W., Gong, Z. H., Hu, M., and Zhu, T.: Highly time-resolved chemical characterization of atmospheric fine particles during 2010 Shanghai World Expo, Atmos. Chem. Phys., 12, 4897-4907, 10.5194/acp-12-4897-2012, 2012.

Knowlton, K., Rosenthal Joyce, E., Hogrefe, C., Lynn, B., Gaffin, S., Goldberg, R., Rosenzweig, C., Civerolo, K., Ku, J.-Y., and Kinney Patrick, L.: Assessing Ozone-Related Health Impacts under a Changing Climate, Environmental Health Perspectives, 112, 1557-1563, 10.1289/ehp.7163, 2004.

Koukouli, M. E., Theys, N., Ding, J., Zyrichidou, I., Mijling, B., Balis, D., and van der A, R. J.: Updated SO2 emission estimates over China using OMI/Aura observations, Atmos. Meas. Tech., 11, 1817-1832, 10.5194/amt-11-1817-2018, 2018.

Kruskal, W. H., and Wallis, W. A.: Use of Ranks in One-Criterion Variance Analysis, Journal of the American Statistical Association, 47, 583-621, 10.2307/2280779, 1952.

Kunshan local chronicles Compilation Committee Office. Kunshan Almanac, Jiangsu Phoenix Science Press, pages 32-35, 2018 (in Chinese).

Li, K., Jacob, D. J., Liao, H., Shen, L., Zhang, Q., and Bates, K. H.: Anthropogenic drivers of 2013–2017 trends in summer surface ozone in China, Proceedings of the National Academy of Sciences, 116, 422-427, 10.1073/pnas.1812168116, 2019.

Mann, H. B.: Nonparametric Tests Against Trend, Econometrica, 13, 245-259, 10.2307/1907187, 1945.

Petit, J. E., Favez, O., Albinet, A., and Canonaco, F.: A user-friendly tool for comprehensive evaluation of the geographical origins of atmospheric pollution: Wind and trajectory analyses, Environ. Modell. Softw., 88, 183-187, http://dx.doi.org/10.1016/j.envsoft.2016.11.022, 2017.

Sen, P. K.: Estimates of the Regression Coefficient Based on Kendall's Tau, Journal of the American Statistical Association, 63, 1379-1389, 10.2307/2285891, 1968.

Shiraiwa, M., Ueda, K., Pozzer, A., Lammel, G., Kampf, C. J., Fushimi, A., Enami, S., Arangio, A. M., Fröhlich-Nowoisky, J., Fujitani, Y., Furuyama, A., Lakey, P. S. J., Lelieveld, J., Lucas, K., Morino, Y.,

Pöschl, U., Takahama, S., Takami, A., Tong, H., Weber, B., Yoshino, A., and Sato, K.: Aerosol Health Effects from Molecular to Global Scales, Environmental Science & Technology, 51, 13545-13567, 10.1021/acs.est.7b04417, 2017.

Sun, Y., Jiang, Q., Wang, Z., Fu, P., Li, J., Yang, T., and Yin, Y.: Investigation of the sources and evolution processes of severe haze pollution in Beijing in January 2013, J. Geophys. Res. Atmos., 119, 4380-4398, 10.1002/2014JD021641, 2014.

Sun, Y., Chen, C., Zhang, Y., Xu, W., Zhou, L., Cheng, X., Zheng, H., Ji, D., Li, J., Tang, X., Fu, P., and Wang, Z.: Rapid formation and evolution of an extreme haze episode in Northern China during winter 2015, Sci. Rep. , 6, 27151, 10.1038/srep27151, 2016a.

Sun, Y., Du, W., Fu, P., Wang, Q., Li, J., Ge, X., Zhang, Q., Zhu, C., Ren, L., Xu, W., Zhao, J., Han, T., Worsnop, D. R., and Wang, Z.: Primary and secondary aerosols in Beijing in winter: sources, variations and processes, Atmos. Chem. Phys., 16, 8309-8329, 10.5194/acp-16-8309-2016, 2016b.

Sun, Y. L., Wang, Z. F., Du, W., Zhang, Q., Wang, Q. Q., Fu, P. Q., Pan, X. L., Li, J., Jayne, J., and Worsnop, D. R.: Long-term real-time measurements of aerosol particle composition in Beijing, China: seasonal variations, meteorological effects, and source analysis, Atmos. Chem. Phys., 15, 14549-14591, 10.5194/acpd-15-14549-2015, 2015.

Tian, H. Z., Wang, Y., Xue, Z. G., Cheng, K., Qu, Y. P., Chai, F. H., and Hao, J. M.: Trend and characteristics of atmospheric emissions of Hg, As, and Se from coal combustion in China, 1980–2007, Atmos. Chem. Phys., 10, 11905-11919, 10.5194/acp-10-11905-2010, 2010.

Waked, A., Favez, O., Alleman, L. Y., Piot, C., Petit, J. E., Delaunay, T., Verlinden, E., Golly, B., Besombes, J. L., Jaffrezo, J. L., and Leoz-Garziandia, E.: Source apportionment of PM₁₀ in a north-western Europe regional urban background site (Lens, France) using positive matrix factorization and including primary biogenic emissions, Atmos. Chem. Phys., 14, 3325-3346, 10.5194/acp-14-3325-2014, 2014.

Wang, G., Zhang, R., Gomez, M. E., Yang, L., Levy Zamora, M., Hu, M., Lin, Y., Peng, J., Guo, S., Meng, J., Li, J., Cheng, C., Hu, T., Ren, Y., Wang, Y., Gao, J., Cao, J., An, Z., Zhou, W., Li, G., Wang, J., Tian, P., Marrero-Ortiz, W., Secrest, J., Du, Z., Zheng, J., Shang, D., Zeng, L., Shao, M., Wang, W., Huang, Y., Wang, Y., Zhu, Y., Li, Y., Hu, J., Pan, B., Cai, L., Cheng, Y., Ji, Y., Zhang, F., Rosenfeld, D., Liss, P. S., Duce, R. A., Kolb, C. E., and Molina, M. J.: Persistent sulfate formation from London Fog to Chinese haze, Proc. Natl. Acad. Sci. U.S.A., 10.1073/pnas.1616540113, 2016a.

Wang, G., Zhang, R., Gomez, M. E., Yang, L., Levy Zamora, M., Hu, M., Lin, Y., Peng, J., Guo, S., Meng, J., Li, J., Cheng, C., Hu, T., Ren, Y., Wang, Y., Gao, J., Cao, J., An, Z., Zhou, W., Li, G., Wang, J., Tian, P., Marrero-Ortiz, W., Secrest, J., Du, Z., Zheng, J., Shang, D., Zeng, L., Shao, M., Wang, W., Huang,

Y., Wang, Y., Zhu, Y., Li, Y., Hu, J., Pan, B., Cai, L., Cheng, Y., Ji, Y., Zhang, F., Rosenfeld, D., Liss, P. S., Duce, R. A., Kolb, C. E., and Molina, M. J.: Persistent sulfate formation from London Fog to Chinese haze, Proceedings of the National Academy of Sciences, 113, 13630-13635, 10.1073/pnas.1616540113, 2016b.

Wang, T., Wang, P., Theys, N., Tong, D., Hendrick, F., Zhang, Q., and Van Roozendael, M.: Spatial and temporal changes in SO2 regimes over China in the recent decade and the driving mechanism, Atmos. Chem. Phys., 18, 18063-18078, 10.5194/acp-18-18063-2018, 2018.

Xie, Y., Ding, A., Nie, W., Mao, H., Qi, X., Huang, X., Xu, Z., Kerminen, V.-M., Petäjä, T., Chi, X., Virkkula, A., Boy, M., Xue, L., Guo, J., Sun, J., Yang, X., Kulmala, M., and Fu, C.: Enhanced sulfate formation by nitrogen dioxide: Implications from in-situ observations at the SORPES Station, J. Geophys. Res.: Atmos., n/a-n/a, 10.1002/2015JD023607, 2015.

Xu, J., Tie, X., Gao, W., Lin, Y., and Fu, Q.: Measurement and model analyses of the ozone variation during 2006 to 2015 and its response to emission change in megacity Shanghai, China, Atmos. Chem. Phys., 19, 9017-9035, 10.5194/acp-19-9017-2019, 2019.

Zhai, S., Jacob, D. J., Wang, X., Shen, L., Li, K., Zhang, Y., Gui, K., Zhao, T., and Liao, H.: Fine particulate matter (PM2.5) trends in China, 2013–2018: contributions from meteorology, Atmos. Chem. Phys. Discuss., 2019, 1-19, 10.5194/acp-2019-279, 2019.

Zhang, Q., Zheng, Y., Tong, D., Shao, M., Wang, S., Zhang, Y., Xu, X., Wang, J., He, H., Liu, W., Ding, Y., Lei, Y., Li, J., Wang, Z., Zhang, X., Wang, Y., Cheng, J., Liu, Y., Shi, Q., Yan, L., Geng, G., Hong, C., Li, M., Liu, F., Zheng, B., Cao, J., Ding, A., Gao, J., Fu, Q., Huo, J., Liu, B., Liu, Z., Yang, F., He, K., and Hao, J.: Drivers of improved PM_{2.5} air quality in China from 2013 to 2017, Proceedings of the National Academy of Sciences, 201907956, 10.1073/pnas.1907956116, 2019a.

Zhang, R., Wang, G., Guo, S., Zamora, M. L., Ying, Q., Lin, Y., Wang, W., Hu, M., and Wang, Y.: Formation of Urban Fine Particulate Matter, Chem. Rev., 115, 3803-3855, 10.1021/acs.chemrev.5b00067, 2015a.

Zhang, Y.-L., and Cao, F.: Fine particulate matter (PM2.5) in China at a city level, Scientific Reports, 5, 14884, 10.1038/srep14884, 2015.

Zhang, Y., Tang, L., Yu, H., Wang, Z., Sun, Y., Qin, W., Chen, W., Chen, C., Ding, A., Wu, J., Ge, S., Chen, C., and Zhou, H.-C.: Chemical composition, sources and evolution processes of aerosol at an urban site in Yangtze River Delta, China during wintertime, Atmos. Environ., 123, Part B, 339-349, http://dx.doi.org/10.1016/j.atmosenv.2015.08.017, 2015b.

Zhang, Y., Tang, L., Croteau, P. L., Favez, O., Sun, Y., Canagaratna, M. R., Wang, Z., Couvidat, F., Albinet, A., Zhang, H., Sciare, J., Prévôt, A. S. H., Jayne, J. T., and Worsnop, D. R.: Field characterization

of the PM2.5 Aerosol Chemical Speciation Monitor: insights into the composition, sources, and processes of fine particles in eastern China, Atmos. Chem. Phys., 17, 14501-14517, 10.5194/acp-17-14501-2017, 2017a.

Zhang, Y., Tang, L., Sun, Y., Favez, O., Canonaco, F., Albinet, A., Couvidat, F., Liu, D., Jayne, J. T., Wang, Z., Croteau, P. L., Canagaratna, M. R., Zhou, H.-C., Prévôt, A. S. H., and Worsnop, D. R.: Limited formation of isoprene epoxydiols-derived secondary organic aerosol under NOx-rich environments in Eastern China, Geophys. Res. Lett., 44, 2035-2043, 10.1002/2016GL072368, 2017b.

Zhang, Y., Favez, O., Petit, J. E., Canonaco, F., Truong, F., Bonnaire, N., Crenn, V., Amodeo, T., Prévôt, A. S. H., Sciare, J., Gros, V., and Albinet, A.: Six-year source apportionment of submicron organic aerosols from near-continuous measurements at SIRTA (Paris area, France), Atmos. Chem. Phys. Discuss., 2019, 1-41, 10.5194/acp-2019-515, 2019b.

Zhang, Y. J., Tang, L. L., Wang, Z., Yu, H. X., Sun, Y. L., Liu, D., Qin, W., Canonaco, F., Prévôt, A. S. H., Zhang, H. L., and Zhou, H. C.: Insights into characteristics, sources, and evolution of submicron aerosols during harvest seasons in the Yangtze River delta region, China, Atmos. Chem. Phys., 15, 1331-1349, 10.5194/acp-15-1331-2015, 2015c.

Zheng, B., Tong, D., Li, M., Liu, F., Hong, C., Geng, G., Li, H., Li, X., Peng, L., Qi, J., Yan, L., Zhang, Y., Zhao, H., Zheng, Y., He, K., and Zhang, Q.: Trends in China's anthropogenic emissions since 2010 as the consequence of clean air actions, Atmos. Chem. Phys., 18, 14095-14111, 10.5194/acp-18-14095-2018, 2018.

Figure 1.

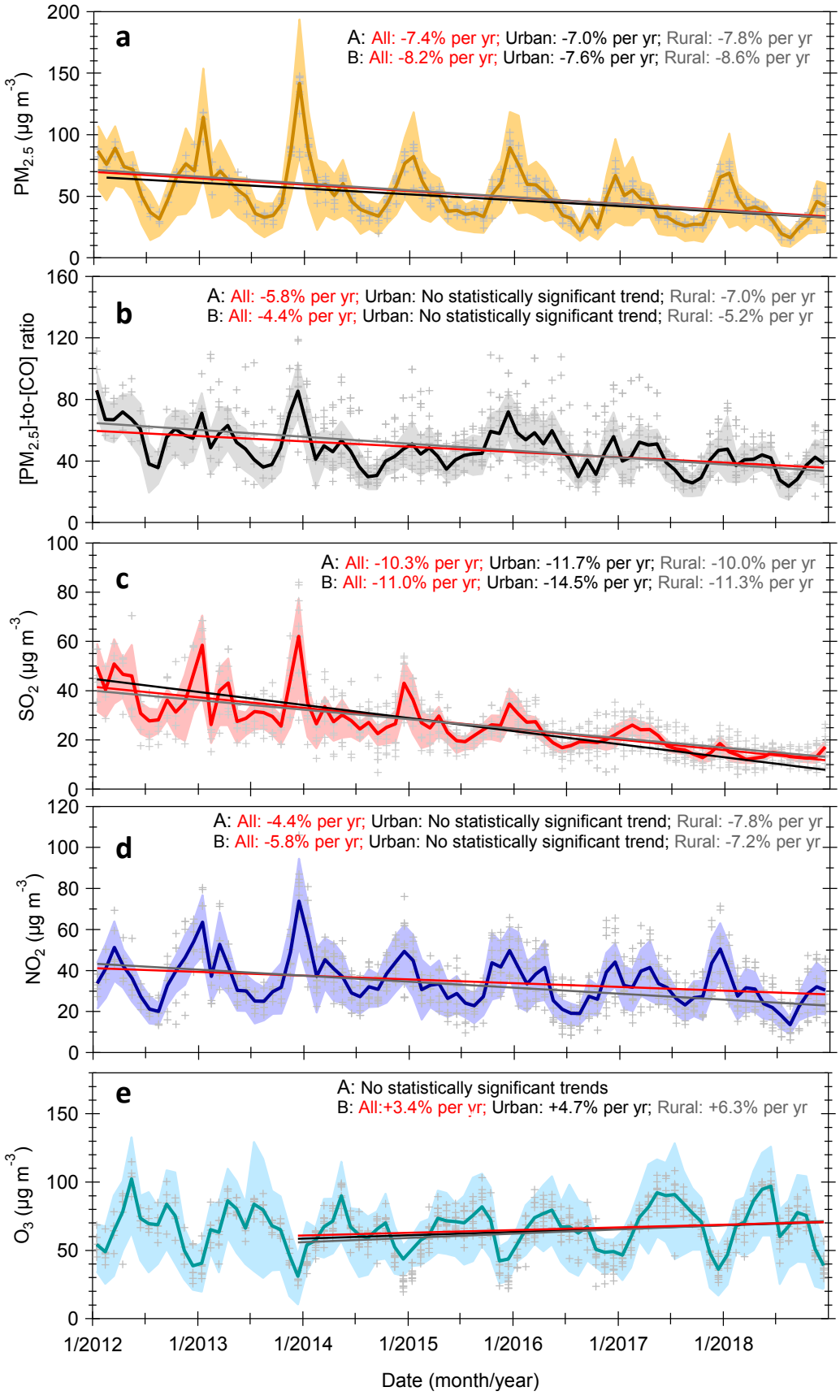
a
A: All: -7.4% per yr; Urban: -7.0% per yr; Rural: -7.8% per yr
B: All: -8.2% per yr; Urban: -7.6% per yr; Rural: -8.6% per yr
PM2.5 (μg m-3)
b
A: All: -5.8% per yr; Urban: No statistically significant trend; Rural: -7.0% per yr
B: All: -4.4% per yr; Urban: No statistically significant trend; Rural: -5.2% per yr
[PM2.5]-to-[CO] ratio
c
A: All: -10.3% per yr; Urban: -11.7% per yr; Rural: -10.0% per yr
B: All: -11.0% per yr; Urban: -14.5% per yr; Rural: -11.3% per yr
SO2 (μg m-3)
d
A: All: -4.4% per yr; Urban: No statistically significant trend; Rural: -7.8% per yr
B: All: -5.8% per yr; Urban: No statistically significant trend; Rural: -7.2% per yr
NO2 (μg m-3)
e
A: No statistically significant trends
B: All:+3.4% per yr; Urban: +4.7% per yr; Rural: +6.3% per yr
O3 (μg m-3)
1/2012
1/2013
1/2014
1/2015
1/2016
1/2017
1/2018
Date (month/year)

Figure 2.

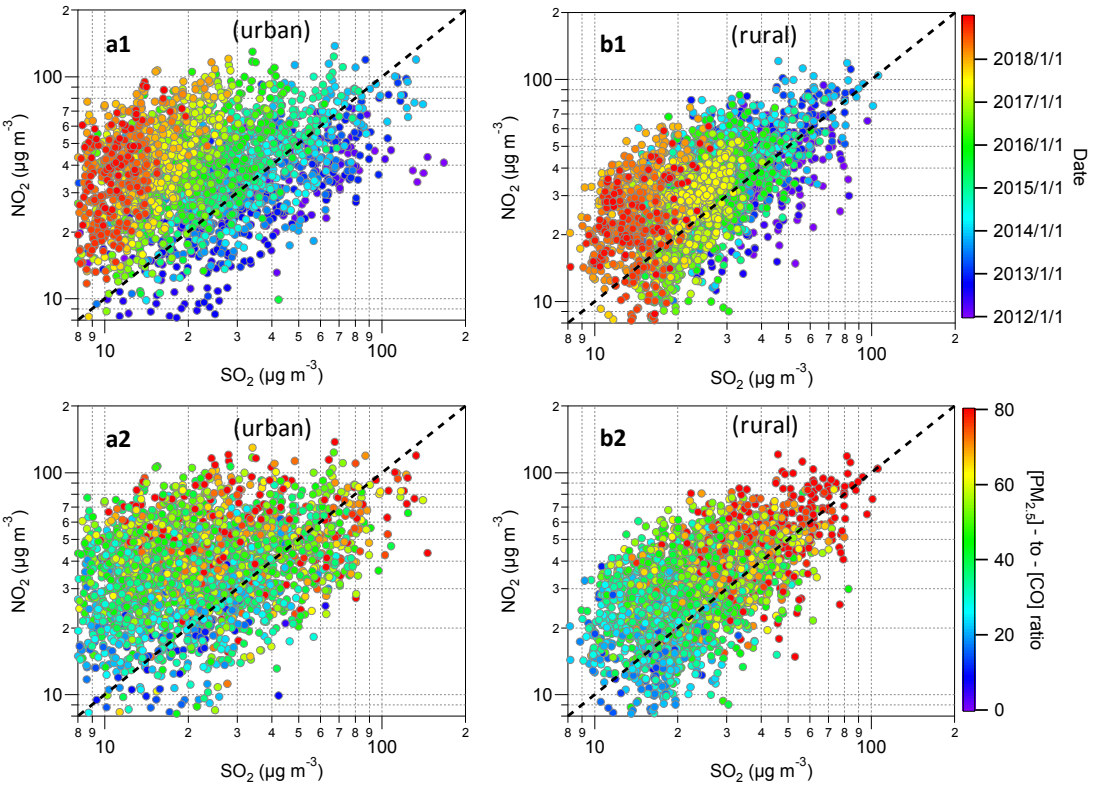
a1
(urban)
b1
(rural)
a2
(urban)
b2
(rural)
NO2 (μg m-3)
SO2 (μg m-3)
Date
2018/1/1
2017/1/1
2016/1/1
2015/1/1
2014/1/1
2013/1/1
2012/1/1
[PM2.5] - to - [CO] ratio
80
60
40
20
0

Figure 3.

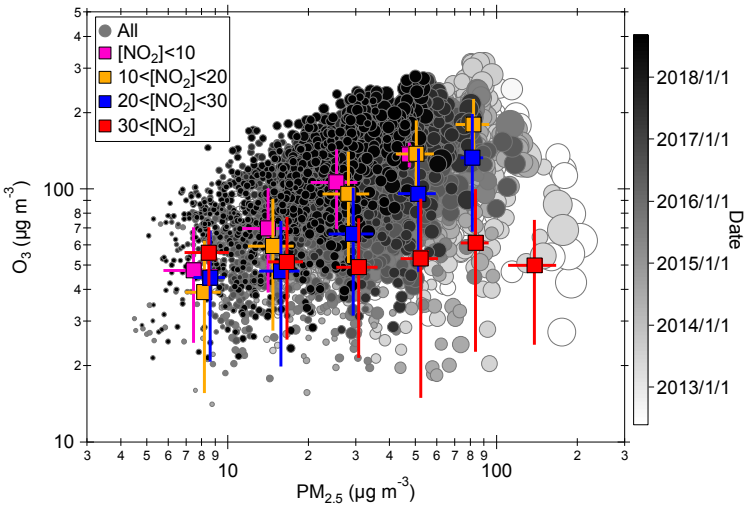
All
[NO2]<10
10<[NO2]<20
20<[NO2]<30
30<[NO2]
O3 (μg m-3)
PM2.5 (μg m-3)
Date
2018/1/1
2017/1/1
2016/1/1
2015/1/1
2014/1/1
2013/1/1

Figure 4.

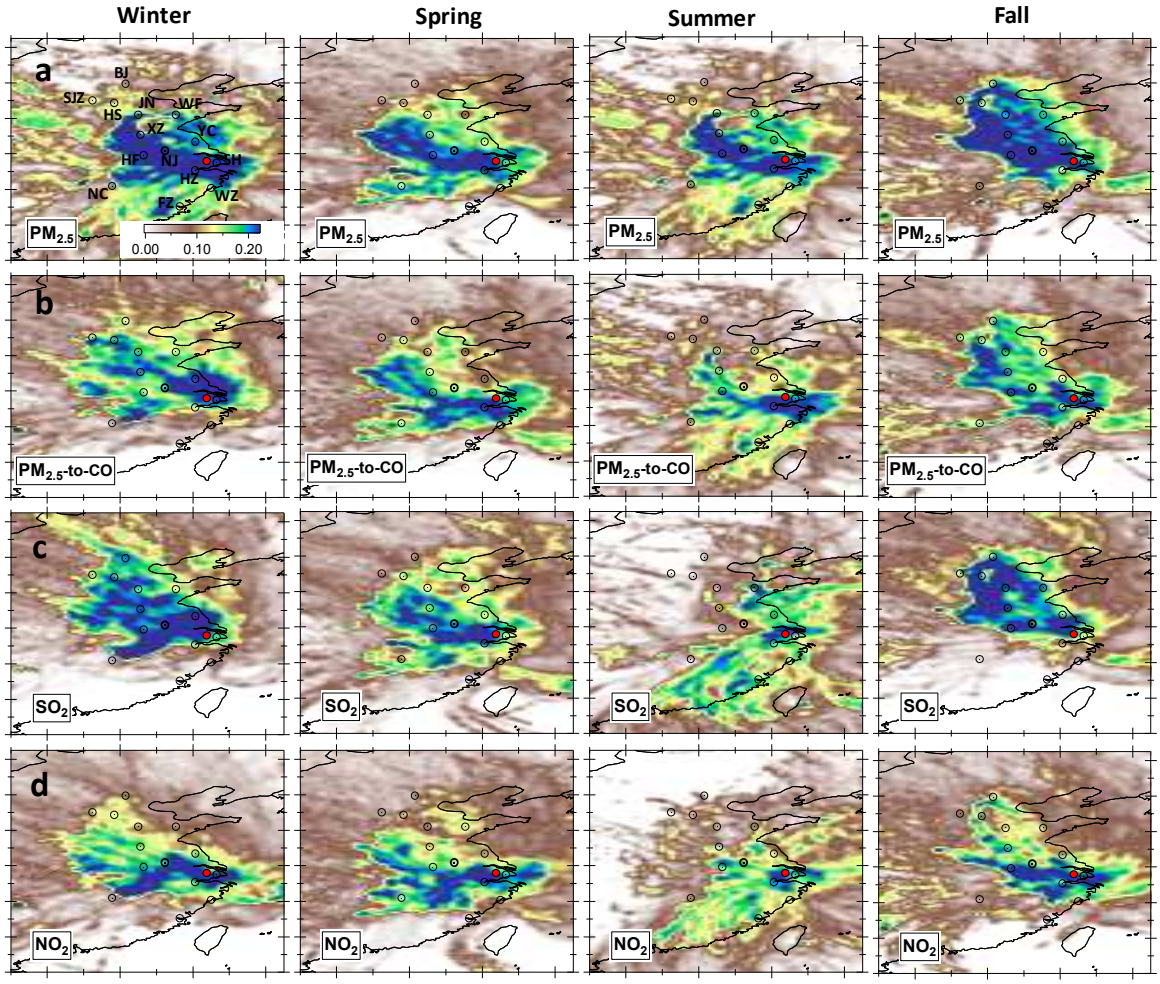
Winter
Spring
Summer
Fall
a
b
c
d
BJ
SJZ
JN
WF
HS
XZ
YC
HF
NJ
SH
HZ
NC
FZ
WZ
0.00
0.10
0.20
PM2.5
PM2.5-to-CO
SO2
NO2

Figure 5.